Engineering Geology 191 (2015) 31–35

Contents lists available at ScienceDirect

Engineering Geology

journal homepage: www.elsevier.com/locate/enggeo

Technical Note

Undrained failure mechanisms of slopes in random soil

H. Zhu [a], D.V. Griffiths [b,c], G.A. Fenton [d], L.M. Zhang [e,*]

[a] Dept. of Civil and Environmental Engineering, The Hong Kong University of Science and Technology, Clear Water Bay, Hong Kong
[b] Dept. of Civil and Environmental Engineering, Colorado School of Mines, Golden, CO 80401, USA
[c] Australian Research Council Centre of Excellence for Geotechnical Science and Engineering, University of Newcastle, Callaghan, NSW 2308, Australia
[d] Dept. of Applied Mathematics, Dalhousie University, Halifax, Nova Scotia, Canada
[e] Dept. of Civil and Environmental Engineering, The Hong Kong University of Science and Technology, Hong Kong

ARTICLE INFO

Article history:
Received 3 December 2014
Received in revised form 12 March 2015
Accepted 17 March 2015
Available online 26 March 2015

Keywords:
Finite element method
Landslides
Shear strength
Slope stability
Stochastic models
Structural reliability

ABSTRACT

Since the charts of Taylor (1937), it has been well known in engineering geological investigations that the location of the critical failure mechanism in a homogeneous undrained clay slope goes either deep (tangent to a firm base) or shallow (through the toe) depending on whether the slope angle is less than or greater than about 53°. In reality, natural soils always exhibit spatial variability and the above expectations no longer hold true. The objective of this note is to investigate the failure mechanisms and probability of failure of slopes in random undrained soil over a wide range of slope angles. An elastic–perfectly plastic finite element method in combination with random field generation, well known as the random finite element method (RFEM), is employed. RFEM represents a powerful tool for slope stability analyses that allow mechanisms to develop naturally within soil masses. It is found that, for certain combinations of random field properties, relatively flat slopes may display a significant number of shallow mechanisms and steeper slopes may display a significant number of deep mechanisms. For a steep slope, the more variable the undrained shear strength, the less likely the slope is to display a toe mechanism. Understanding the uncertainty of failure mechanisms is important because the consequences may be more serious in a deep failure as it involves a greater volume of soil.

1. Introduction

Landslide risk assessment involves the probability of failure and the consequences of failure (e.g. Christian, 2004; Ang and Tang, 2007; Fenton and Griffiths, 2008; Khoshnevisan et al., 2014; Zhang et al., 2014c). The probability of failure (p_f) can be estimated from engineering analysis but the consequences of failure are site-specific (e.g. loss of life and properties). As shown by the two slopes in Fig. 1, both cases have failed, but the volume of sliding soil at the initiation of a landslide is clearly different. The deeper failure mechanism can be assumed to be more serious, because a greater volume of soil is involved.

Since the charts of Taylor (1937), it has been well known that the location of the critical failure mechanism in a homogeneous undrained clay slope goes either deep (tangent to a firm base) or shallow (through the toe) depending on whether the slope angle is less than or greater than about 53°. When slopes are made up of variable soil, however, these expectations no longer hold true. Indeed soil shear strength properties can vary significantly from point to point (e.g., Li et al., 2009; Li and Zhang, 2010; Cao and Wang, 2013; Juang et al., 2013; Lacasse et al., 2013; Zhao et al., 2013; Zhang et al., 2014a), and the failure mechanisms are also uncertain.

The random finite element method (RFEM) offers a systematic way of accounting for spatial variability. The RFEM, which combines finite elements with random fields generated to account for spatial variation, has been applied successfully to slope reliability analysis (e.g., Griffiths and Fenton, 2000, 2004; Fenton et al., 2013; Ali et al., 2014; Jiang et al., 2014; Le, 2014; Lloret-Cabot et al., 2014; Zhang et al., 2014b). RFEM not only estimates the value of p_f but also delivers useful visualisations of the failure mechanism and displacement vectors. A significant advantage of RFEM is that it allows failure mechanisms to develop naturally through soil masses by following the path of least resistance.

The objective of this note is to investigate the failure mechanisms and probability of failure of slopes in random undrained soil over a wide range of slope angles. While the detailed assessment of runout characteristics and failure consequences is beyond the scope of this note, the fraction of failures which are deep vs. shallow is presented for various slope angles and soil statistics. This allows the reader to perform at least a qualitative assessment of landslide risk assessment as a function of slope angle and soil variability.

A test slope in undrained clay is considered in this note and the geometry and input parameters of the slope are shown in Fig. 2. The slope has an embankment depth of $H = 10$ m and a foundation to

* Corresponding author.
E-mail addresses: zhuhong@ust.hk (H. Zhu), d.v.griffiths@mines.edu (D.V. Griffiths), gordon.fenton@dal.ca (G.A. Fenton), cezhangl@ust.hk (L.M. Zhang).

http://dx.doi.org/10.1016/j.enggeo.2015.03.009
0013-7952/

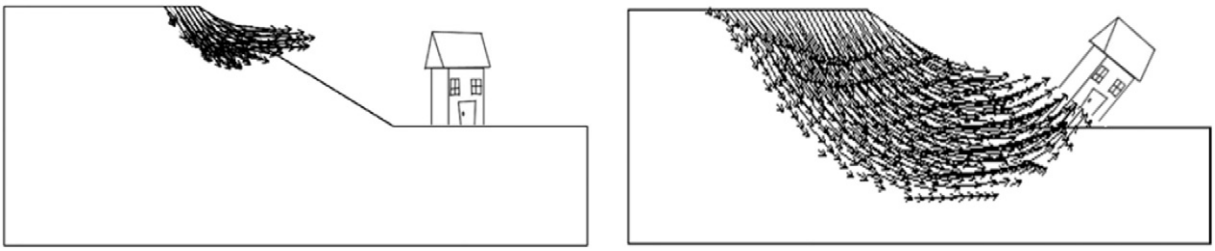

Fig. 1. Shallow and deep failure mechanisms in a stratified soil. Both cases have failed, but the consequences are clearly different.

depth ratio of $DH = 1.5H$. The slope geometry given by H, D, β and saturated unit weight γ_{sat} are assumed to be deterministic, but the undrained shear strength, c_u, is taken as a spatially varying random variable. The values of these parameters are summarized in Table 1. c_u is non-dimensionalized as $C = c_u/(\gamma_{sat}H)$ and characterized by a lognormal distribution defined by a mean (μ_C), a standard deviation (σ_C) and a spatial correlation length ($\theta_{\ln C}$).

A mechanism that goes through the toe but not tangent to the firm base is called a toe failure mechanism. One that goes deep tangent to the firm base and outcrops at the foundation layer is called a deep failure mechanism. Other mechanisms are entirely above the toe. The toe and deep failure mechanisms displayed in deterministic soil are shown in Fig. 3. The vertical cut ($\beta = 90$ °) and a flatter slope ($\beta = 30$ °) are selected as typical examples.

This note first describes issues on failure mechanisms and probability of failure of slopes in random undrained soil and then introduces briefly the random finite element method for slope stability analysis. Subsequently, the influence of slope angle on failure mechanism and location in undrained soil is presented in detail. Various coefficients of variation of undrained shear strength are considered. The proportions of toe failure mechanisms are examined. Finally, key conclusions are drawn.

2. Brief introduction to the RFEM

The slope stability analysis uses an elastic–perfectly plastic stress–strain law with a Mohr–Coulomb failure criterion. It involves applying gravity loading and monitoring the stresses at all the Gauss points. If the Mohr–Coulomb criterion at a Gauss point is violated, the algorithm will try to redistribute the stresses to neighbouring elements that still have reserves of shear strength. This is an iterative process that continues until both the Mohr–Coulomb criterion and the global equilibrium are satisfied at all Gauss points. In this study, failure is said to have occurred if the algorithm is unable to satisfy these criteria within an iteration ceiling, typically set to 500.

The undrained shear strength, c_u, is considered as a spatially varying random variable and the distribution of c_u in the slope domain (Fig. 2) is simulated as an isotropic random field. The non-dimensionalized shear strength parameter, C, is assumed to follow a lognormal distribution. The lognormal distribution guarantees that all the random variables are non-negative and benefits from a simple transformation to the classical

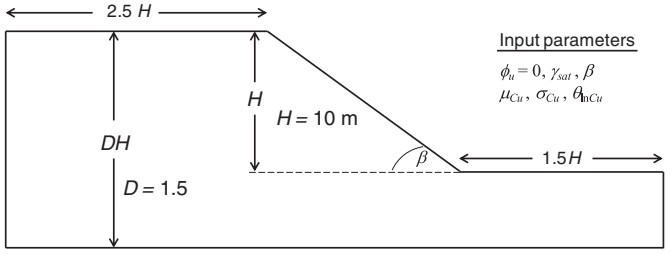

Fig. 2. Geometry and input parameters for the test slope.

normal (Gaussian) distribution. It has been used and advocated by many researchers as a reasonable model for soil properties (e.g. Lacasse et al., 2013). The coefficient of variation, ν_C, given by

$$\nu_C = \frac{\sigma_C}{\mu_C} \tag{1}$$

is a useful guide to the dispersion of the distribution about the mean. The value of ν_C for undrained shear strength varies from small values to up to 0.6 (e.g. Ching and Phoon, 2013).

In addition to μ_C and ν_C, the spatial correlation length ($\theta_{\ln C}$) can be included to describe the correlation between random variables at two spatial locations. The correlation length denotes the distance over which random values tend to be correlated. In the interests of generality, the correlation length has been non-dimensionalized by dividing it by the slope height (Fig. 2) as follows:

$$\Theta = \theta_{\ln C}/H. \tag{2}$$

The spatial correlation length is assumed isotropic throughout this note and soil anisotropy is not considered (e.g. Zhu and Zhang, 2013). An exponential decaying autocorrelation function of the following form is used:

$$\rho = \exp(-2\tau/\theta_{\ln C}) \tag{3}$$

where $\rho$is the correlation coefficient and τ is the absolute distance between two points in a random field. The correlation function describes spatial persistence, i.e. soil samples taken close together are more likely to have similar properties than if they are far apart.

A large number of realizations of the random field are generated, each having the same statistics but differing in the locations of strong and weak soils. A deterministic finite element analysis is conducted for each realization of random field. In the context of RFEM, each element within each realization of the Monte-Carlo process is assigned a constant, but random, soil property. The statistics of the assigned value are affected by the size of the element. The statistics of the underlying log field due to local averaging are given by

$$\sigma_{\ln C_A} = \sigma_{\ln C}\sqrt{\Gamma} \tag{4a}$$

$$\mu_{\ln C_A} = \mu_{\ln C} \tag{4b}$$

Table 1
Summary of input parameters for the test slope.

Parameter	Definition	Value
H (m)	Slope height	10
D	Foundation depth ratio	1.5
β (°)	Slope angle	10–90
c_u (kN/m^2)	Undrained cohesion	Random variable
ϕ_u (°)	Undrained friction angle	0
γ_{sat} (kN/m^3)	Saturated unit weight	20
ψ (°)	Dilation angle	0
E (kN/m^2)	Young's modulus	10^5

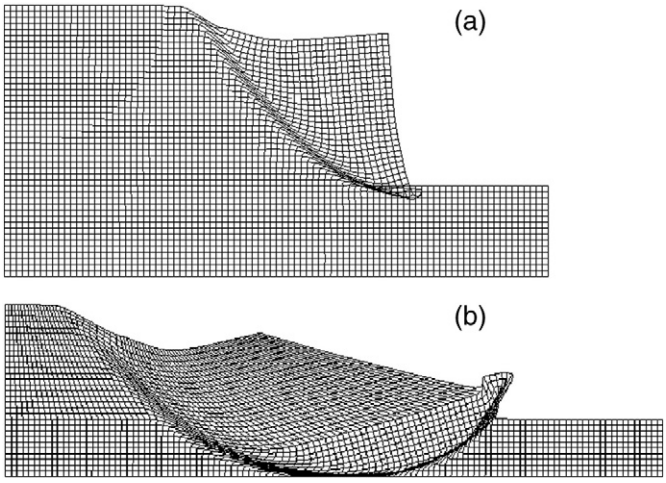

Fig. 3. Definition of toe and deep failure mechanisms: (a) vertical cut ($\beta = 90$ °); and (b) flatter slope ($\beta = 30$ °).

where Γ is the variance reduction factor ranging between 0 and 1. Eqs. (4a) and (4b) lead to the following statistics of log-normal field, which are mapped onto the finite-element mesh,

$$\mu_{C_A} = \exp\left(\mu_{\ln C_A} + \frac{1}{2}\sigma^2_{\ln C_A}\right) \tag{5a}$$

$$\sigma_{C_A} = \mu_{C_A}\sqrt{\exp\left(\sigma^2_{\ln C_A}\right) - 1}. \tag{5b}$$

If the distribution of the random variable is normal, local averaging over the element reduces the variance but the mean is unaffected. If a lognormal distribution is assumed, as is the case here, both the mean and the variance are reduced by local averaging (e.g. Griffiths and Fenton, 2001). Adjustment to the statistics due to local averaging should be implemented prior to generating the random field used to map shear strengths to their associated finite elements. The local averaging over the elements and subsequent random field generation is accomplished by using the Local Average Subdivision method developed by Fenton and Vanmarcke (1990). Following a sufficient number of Monte-Carlo simulations, the p_f is obtained as the proportion of the total number of simulations that required 500 iterations or more.

In this note, a range of non-dimensionalized spatial correlation lengths and different v_C values are considered. 2000 simulations are determined to be sufficient to give a reliable and reproducible estimate of p_f in each analysis case. The standard error of the estimate is $\sigma_{p_f} = \sqrt{p_f\left(1-p_f\right)/n}$, where n is the number of simulations (Fenton et al., 2013). σ_{p_f} is 0.0067 when n is 2000 and p_f is 0.1. In the following two sections, results of the RFEM analyses are presented to demonstrate the influence of slope angle on the p_f and failure mechanisms of slopes in random undrained clay.

3. Probabilistic stability analysis of the test slope

In this section we present results of RFEM analysis on the test slope in Fig. 2 for a range of slope angles (β) and coefficients of variation of undrained strength (v_C). Fig. 4 shows that, for a typical range of v_C values with $\Theta = 0.5$, the greater the value of v_C, the greater the value of p_f for all slope angles considered. Fig. 5 demonstrates that, with fixed values of $DH = 1.5H$, $\mu_C = 0.2$ and $\Theta = 0.5$, a $\beta = 30$ ° slope with a deterministic factor of safety of 1.2 (based on the mean) can result in a p_f as high as 0.38. It should be noted that a factor of safety based on the mean strength of a variable soil would generally lead to optimistic estimates of the level of safety. A lower value of the characteristic strength would typically be used in practice as discussed by Griffiths and Fenton (2004). Fig. 5 also demonstrates that for the cases considered, the probability of failure becomes vanishingly small when the factor of safety is approximately greater than 1.4 and 1.6, respectively, for $v_C = 0.2$ and 0.4.

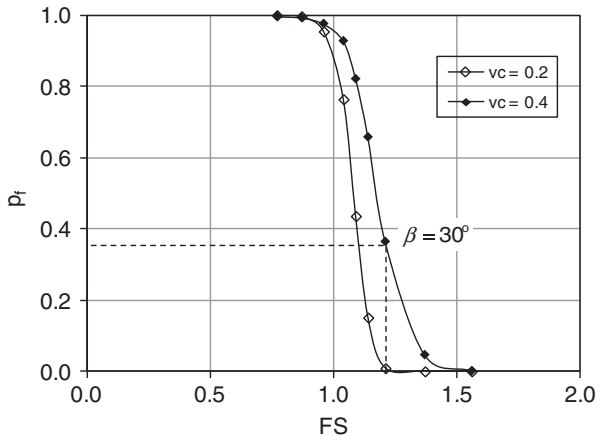

Fig. 4. Probability of failure versus deterministic factor of safety (based on the mean) of undrained slopes. $DH = 1.5H$, $\mu_C = 0.2$ and $\Theta = 0.5$.

Fig. 6 shows the relationships between p_f and slope angle for various correlation lengths. All the analysis cases in Fig. 6 are subjected to the condition of $DH = 1.5H$, $\mu_C = 0.2$ and $v_C = 0.2$. For all correlation lengths, p_f increases with increasing slope angle, which is expected. However, the failure probability is two-tailed when Θ tends to 0: p_f tends to 1 for slope angles greater than about 48° but tends to 0 for slope angles less than about 48°. The findings emphasize the importance of the slope angle in the relationship between p_f and Θ. Including the spatial soil variability helps quantify the chance of "non-failure" of very steep slopes.

4. Failure mechanisms

Fig. 7 shows undeformed and deformed meshes at failure for several combinations of parameters. Unlike the deterministic case, when the slope consists of spatially random soil, a vertical cut may display a deep mechanism (Fig. 7(g)) and a flat slope may display a shallow mechanism (Fig. 7(h)). Following each set of Monte-Carlo simulations,

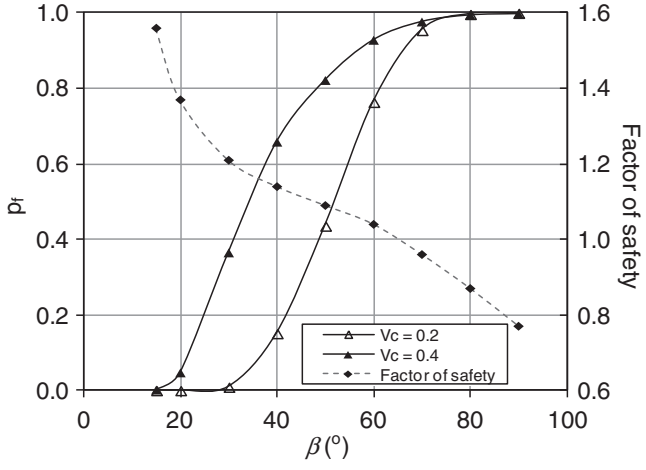

Fig. 5. Probability of failure and deterministic factor of safety (based on the mean) versus slope angle of undrained slopes. $DH = 1.5H$, $\mu_C = 0.2$ and $\Theta = 0.5$.

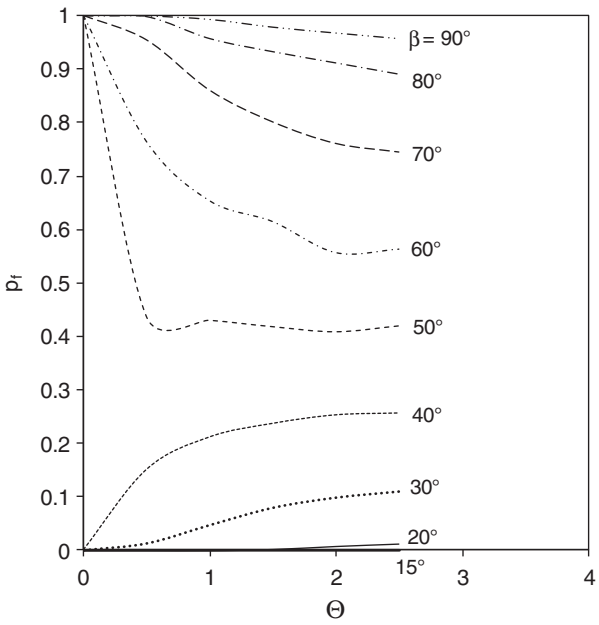

Fig. 6. Influence of slope angle on the probability of failure of undrained slopes. $DH = 1.5H$, $\mu_C = 0.2$ and $\nu_C = 0.2$.

the proportion of toe failure mechanisms defined earlier (ratio of the number of toe failure mechanisms to the total number of failure simulations) has been recorded.

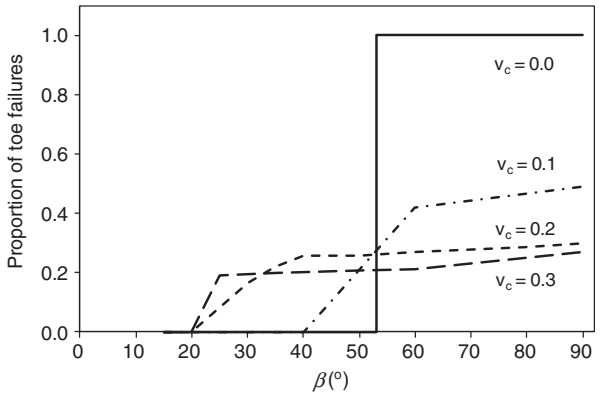

Fig. 8. Proportion of toe failures versus slope angle of undrained slopes. $DH = 1.5H$, $\mu_C = 0.2$ and $\Theta = 0.5$.

Fig. 8 shows the proportion of toe failures as a function of slope angle for a range of coefficients of variation of undrained shear strength at a fixed correlation length. The step-function result corresponding to $\nu_C = 0$ is based on the $\beta = 53°$ transition point indicated by Taylor's chart. For random undrained vertical cuts ($\beta = 90°$), a significant number of deep failure mechanisms are observed when weaker soil is present in the deeper foundation layer, and for flatter slopes ($\beta = 30°$), a significant number of toe mechanisms are observed when weaker soil is present in the shallower embankment zone. Fig. 8 also shows that for all ν_C values, the proportion of toe mechanisms increases with increasing slope angle but tends to flatten out at high slope angles. For example, the rate of increase of toe failures reduces significantly at

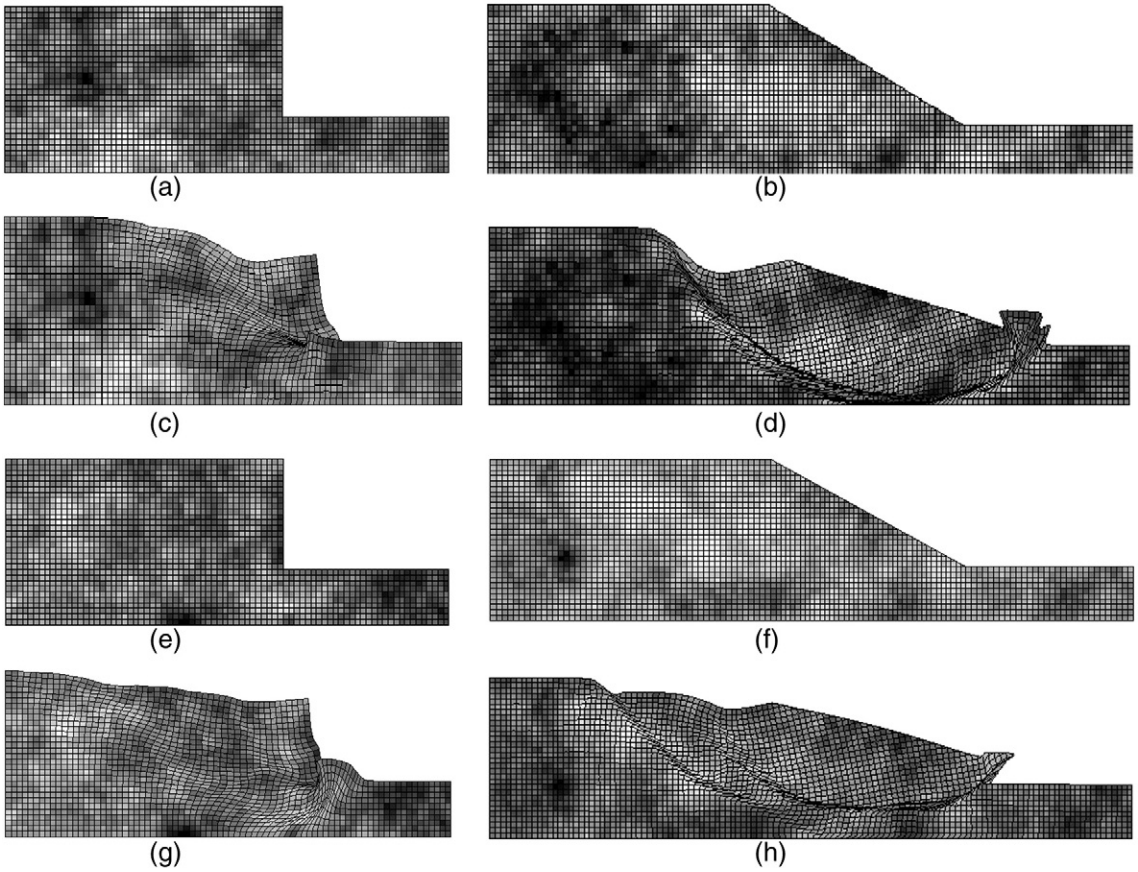

Fig. 7. Failure mechanism of undrained slope with fixed $C = 0.2$ and $\Theta = 0.5$. Undeformed mesh: (a) $\mu_C = 0.2$, $\nu_C = 0.2$ and $\beta = 90°$ and (b) $\mu_C = 0.2$, $\nu_C = 0.2$ and $\beta = 30°$; deformed mesh at failure: (c) $\mu_C = 0.2$, $\nu_C = 0.2$ and $\beta = 90°$ and (d) $\mu_C = 0.2$, $\nu_C = 0.2$ and $\beta = 30°$; undeformed mesh: (e) $\mu_C = 0.2$, $\nu_C = 0.3$ and $\beta = 90°$ and (f) $\mu_C = 0.2$, $\nu_C = 0.3$ and $\beta = 30°$; deformed mesh at failure: (g) $\mu_C = 0.2$, $\nu_C = 0.3$ and $\beta = 90°$ and (h) $\mu_C = 0.2$, $\nu_C = 0.3$ and $\beta = 30°$.

$\beta = 60°$ for $v_C = 0.1$, $\beta = 40°$ for $v_C = 0.2$ and $\beta = 25°$ for $v_C = 0.3$. For higher slope angles, the more variable the undrained shear strength, the smaller the proportion of toe mechanisms that the slope will display. It is expected that, with a wider distribution of the strength due to a greater v_C, weaker soil is more likely to be situated at the deeper foundation layer.

5. Conclusions

This note investigates the failure mechanisms and probability of failure of undrained slopes in spatially random soil modelled by an isotropic random field. The following conclusions can be drawn:

1. The importance of the slope angle, β, on the relationship between p_f and the non-dimensionalized spatial correlation length, Θ, is emphasized. For the test slope, as $\Theta \to 0$, $p_f \to 1$ when $\beta > 48°$ and $p_f \to 0$ when $\beta < 48$ °. The impact of this phenomenon on engineers' risk perception should be noted.
2. For random undrained vertical cuts ($\beta = 90$ °), a significant number of deep failure mechanisms are observed when weaker soil occurs in the foundation layer; and for flatter slopes ($\beta = 30$ °), a significant number of toe mechanisms are observed when weaker soil occurs in the shallower embankment zone.
3. The proportion of toe mechanisms increases with increasing slope angle β until tending to flatten out at higher values of β.
4. For higher slope angles, the more variable the undrained shear strength, the less likely the slope is to display a toe mechanism.

Notation

The following symbols are used in this note:

H	slope height
D	foundation depth ratio
β	slope angle
γ_{sat}	saturated soil unit weight
c_u	undrained shear strength
C	non-dimensionalized undrained shear strength
μ_C	mean of C
σ_C	standard deviation of C
$\theta_{\ln C}$	spatial correlation length of ln C
v_C	coefficient of variation of C
Θ	non-dimensionalized spatial correlation length
p_f	probability of failure

Acknowledgements

The authors wish to thank the Research Grants Council, University Grants Committee, Hong Kong (No. HKUST6/CRF/12R), the National Basic Research Program (No. 2011CB013506) and the Centre of Excellence for Geotechnical Science and Engineering, University of Newcastle Australia.

References

Ali, A., Huang, J.S., Lyamina, A.V., Sloana, S.W., Griffiths, D.V., Cassidy, M.J., Li, J.H., 2014. Simplified quantitative risk assessment of rainfall-induced landslides modelled by infinite slopes. Eng. Geol. 179 (4), 102–116.
Ang, A.H.S., Tang, W.H., 2007. Probability concepts in engineering: emphasis on applications to civil and environmental engineering. 2nd ed. Decision, Risk, and Reliability vol. II. Wiley, New York.
Cao, Z.J., Wang, Y., 2013. Bayesian approach for probabilistic site characterization using cone penetration tests. J. Geotech. Geoenviron. 139 (2), 267–276.
Ching, J.Y., Phoon, K.K., 2013. Multivariate distribution for undrained shear strengths under various test procedures. Can. Geotech. J. 50 (9), 907–923.
Christian, J.T., 2004. Geotechnical engineering reliability: how well do we know what we are doing? J. Geotech. Geoenviron. 130, 985–1003.
Fenton, G.A., Griffiths, D.V., 2008. Risk Assessment in Geotechnical Engineering. John Wiley & Sons, New York.
Fenton, G.A., Vanmarcke, E.H., 1990. Simulation of random fields via local average subdivision. J. Eng. Mech. 116 (8), 1733–1749.
Fenton, G.A., Hicks, M.A., Wang, X., Griffiths, D.V., 2013. Effect of slope height and gradient on failure probability. Geo-Congress 2013: Stability and Performance of Slopes and Embankments III. ASCE, Reston, pp. 972–981 GSP 231.
Griffiths, D.V., Fenton, G.A., 2000. Influence of soil strength spatial variability on the stability of an undrained clay slope by finite elements. Slope Stability. Geotechnical Special Publication, No. 101. ASCE, Reston, pp. 184–193.
Griffiths, D.V., Fenton, G.A., 2001. Bearing capacity of spatially random soil: the undrained clay Prandtl problem revisited. Geotechnique 51 (4), 351–359.
Griffiths, D.V., Fenton, G.A., 2004. Probabilistic slope stability analysis by finite elements. J. Geotech. Geoenviron. 130 (5), 507–518.
Jiang, S.H., Li, D.Q., Zhang, L.M., Zhou, C.B., 2014. Slope reliability analysis considering spatially variable shear strength parameters using a non-intrusive stochastic finite element method. Eng. Geol. 168, 120–128.
Juang, C.H., Ching, J.Y., Luo, Z., 2013. Assessing SPT-based probabilistic models for liquefaction potential evaluation: a 10-year update. Georisk 7 (3), 137–150.
Khoshnevisan, S., Gong, W.P., Wang, L., Juang, C.H., 2014. Robust design in geotechnical engineering — an update. Georisk 8 (4), 217–234.
Lacasse, S., Hoeg, K., Liu, Z.Q., Nadim, F., 2013. An homage to Wilson Tang: reliability and risk in geotechnical practice — how Wilson led the way. Geotechnical Safety and Risk IV, Hong Kong, 4–6 Dec. 2013. CRC Press, London, pp. 3–26.
Le, T.M.H., 2014. Reliability of heterogeneous slopes with cross-correlated shear strength parameters. Georisk 8 (4), 250–257.
Li, J.H., Zhang, L.M., 2010. Geometric parameters and REV of a crack network in soil. Comput. Geotech. 37 (4), 466–475.
Li, J.H., Zhang, L.M., Wang, Y., Fredlund, D.G., 2009. Permeability tensor and REV of saturated cracked soil. Can. Geotech. J. 46 (8), 928–942.
Lloret-Cabot, M., Fenton, G.A., Hicks, M.A., 2014. On the estimation of scale of fluctuation in geostatistics. Georisk 8 (2), 129–140.
Taylor, D.W., 1937. Stability of earth slopes. J. Boston Soc. Civ. Eng. 24 (3), 337–386.
Zhang, J., Li, J.P., Zhang, L.M., Huang, H.W., 2014a. Calibrating cross-site variability for reliability-based design of pile foundations. Comput. Geotech. 62, 154–163.
Zhang, J., Huang, H.W., Zhang, L.M., Zhu, H.H., Shi, B., 2014b. Probabilistic prediction of rainfall-induced slope failure using a mechanics-based model. Eng. Geol. 168, 129–140.
Zhang, L.M., Zhang, S., Huang, R.Q., 2014c. Multi-hazard scenarios and consequences in Beichuan, China: the first five years after the 2008 Wenchuan earthquake. Eng. Geol. 180, 4–20.
Zhao, H.F., Zhang, L.M., Xu, Y., Chang, D.S., 2013. Variability of geotechnical properties of a fresh landslide soil deposit. Eng. Geol. 166, 1–10.
Zhu, H., Zhang, L.M., 2013. Characterizing geotechnical anisotropic spatial variations using random field theory. Can. Geotech. J. 50 (7), 723–734.